Landscape and Urban Planning 212 (2021) 104107

Contents lists available at ScienceDirect

Landscape and Urban Planning

journal homepage: www.elsevier.com/locate/landurbplan

Research Paper

Understanding temperature related health risk in context of urban land use changes

Vidhee Avashia [a,*], Amit Garg [a], Hem Dholakia [b]

[a] Indian Institute of Management Ahmedabad, Vastrapur, Ahmedabad 380 015, Gujarat, India
[b] Coalition for Disaster Resilient Infrastructure (CDRI), New Delhi, India

HIGHLIGHTS

- Cities are heterogeneous entities with varying microclimates.
- The paper explores role of land use in temperature-mortality relations.
- Land surface and air temperatures show significantly different mortality risks.
- Land use mix has an impact on heat induced relative mortality risks.
- Increased built-up spaces indicates higher temperature induced mortality risks.

GRAPHICAL ABSTRACT

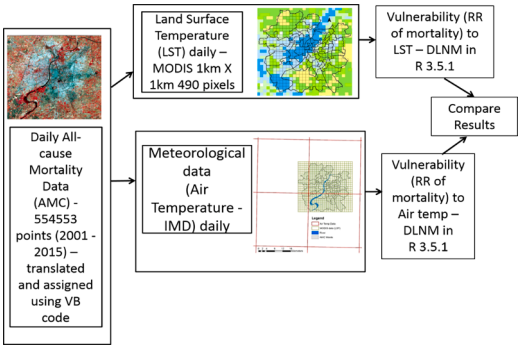

ABSTRACT

A city's climate is affected both by global warming and the local factors such as built form and the landscape. The temperature related impacts of climate change make urban areas more vulnerable particularly due to higher population concentration as well as heat island effect. Cities in India are already experiencing enhanced temperature and precipitation related impacts of climate change and extreme events, e.g., >2 °C warming in some places. This study describes a case of Ahmedabad – a city of around 5 million people (Census, 2011) and currently almost 7.8 million, located in the hot and humid western part of India to understand the current temperature-related mortality impacts and the role of land use. Satellite images (MODIS from NASA), temperature data from India Meteorological Department (IMD) and daily all-cause mortality from Ahmedabad Municipal Corporation between 2001 and 2015 have been used to create a distributed lag non-linear model. Using land surface temperature for mortality risk assessment gives significantly different results as compared to using air temperature for mortality risk assessment. This indicates impacts of localized temperature variations on mortality risks. Thus, the microclimate in a city as represented by land surface temperatures is a better indicator for estimating relative risk of temperature related mortality as compared to air temperature. The study also infers that with increase in built-up spaces by 1% in the land use mix, the relative risk of heat related mortality increases by 0.59 points at 40 °C and by 0.78 points at 45 °C.

1. Introduction

The fifth IPCC assessment report reiterates that several urban areas across the globe will be exposed to temperature rises of 1.5 °C or more, compared with pre-industrial levels, by 2050 (Revi et al., 2014). The temperature-related impact of climate change will make urban areas particularly vulnerable, due to their higher population concentrations and the heat-island effect. Furthermore, climate change is expected to

* Corresponding author.
E-mail address: vidhee@iima.ac.in (V. Avashia).

https://doi.org/10.1016/j.landurbplan.2021.104107
Received 23 May 2020; Received in revised form 17 March 2021; Accepted 28 March 2021
Available online 15 April 2021

exacerbate urban heat islands (UHI) in cities worldwide (Manoli et al., 2019) – indicating that land use and land cover play an important role in determining the temperature-related impacts of climate change. Cities are heterogeneous entities, with different neighbourhoods experiencing different microclimates. Studies suggest that land uses, such as urban green spaces, have a role to play in city-specific climate-change adaptation measures (Sánchez, Solecki, & Batalla, 2018; Rosenzweig, et al., 2015).

Research on global-warming projections for India suggests that air temperature may increase by as much as 3–4 °C towards the end of the 21st century. This warming is likely to be widespread across the country and more pronounced in northern parts of India (Chaturvedi, Joshi, Jayaraman, Bala, & Ravindranath, 2012; IITM, 2012). A recent study suggests that 1- and 3-day concurrent hot day/hot night (CHDHN) events increased significantly in India between 1984 and 2016, in comparison to 1951–1983 (Mukherjee & Mishra, 2018). CHDHN events occur when the temperature of the day/night exceeds the 90th percentile climatologically (Vogel, Zscheischler, Wartenburger, Dee, & Seneviratne, 2019). This makes Indian cities very vulnerable to heat-related temperature stresses. Both the number of hot days and the frequency of heatwaves are expected to increase due to climate change, leading to heat-induced health impacts and mortality. The present study attempts to understand current temperature-related mortality impacts and the role played by land use in mitigating or exacerbating those impacts, using Ahmedabad city, India as a case study.

2. Literature review

A large number of deaths and hospitalisations have been associated with exposure to higher temperatures (Basu & Samet, 2002). One formative work on the association between mortality and extreme temperature investigated 86 US cities between 1925 and 1937, showing that an increase in mortality was preceded by several successive days of extreme temperature (Gover, 1938). Epidemiologists and public-health researchers have undertaken several studies to explore temperature-related mortality across the globe. Many of these studies are time-series statistical associations of daily mortality values with daily ambient temperatures, focusing on extreme temperature conditions (Gasparrini, et al., 2015; Bennett, Blangiardo, Fecht, Elliott, & Ezzati, 2014; Anderson & Bell, 2009; Basu & Ostro, 2008; Curriero, et al., 2002). Given growing concerns about the impact of climate change on health, research has also focused on future mortality risks. A review paper on future mortality-risk assessments, due to higher ambient temperatures, reviewed 63 articles, finding that most studies focused on cities in Canada, the US, Europe, South Korea, and Australia (Sanderson, Arbuthnott, Kovats, Hajat, & Falloon, 2017).

Su et al. (2016) have discussed linkages between public health and land use and landscape planning in the literature on developed countries (Su, Zhang, Pi, Wan, & Weng, 2016). Brown et al. (2015) have shown that evidence-based climate-responsive park design leads to greater thermal comfort (Brown, Vanos, Kenny, & Lenzholzer, 2015). Masoudi and Tan (2019) have established the role of urban green spaces in lowering land-surface temperature (Masoudi & Tan, 2019). Stone et al. (2010) have attempted to link the urban form and extreme-heat events to establish vulnerability to the changing climate through an analysis of 53 large metropolitan cities in the US (Stone, Hess, & Frumkin, 2010). They conclude that the design and management of urban land-use plays a major role in shaping the temperature-related health effects of climate change; they also discuss the implications of this finding and offer adaptation suggestions. Wolf & McGregor (2013) have established a heat-vulnerability index to investigate intra-urban variability within the Greater London area (Wolf & McGregor, 2013). This index, developed using nine proxy variables to establish exposure to heat and sensitivity, has helped them identify the drivers of spatial patterns of heat vulnerability. Such studies can inform in devicing adaptation policies at sub-local levels.

A study carried out in Seoul, South Korea on heat-related mortality and urban vegetation found that areas with less vegetation exhibited a higher mortality risk at high temperatures (Ji-Young, Lane, Jong-Tae, & Bell, 2016). Vargo et al. (2016) have examined the benefits of increased vegetation in three US cities by analysing temperature-related mortality risks. They have shown that age, income, and race play a role in determining the effectiveness of heat management strategies (Vargo, Stone, Habeeb, Liu, & Russell, 2016). In their paper on Berlin, Dugord et al. (2014) have examined the relationship between urban land use, land-surface temperature and the distribution of associated risks (Dugord, Lauf, Schuster, & Kleinschmit, 2014). Similarly, Weber et al. (2015) have discussed extreme-heat vulnerability in Philadelphia, using land- and satellite-based surface-temperature data. They have identified indicators that help to determine Exposure, Sensitivity, Vulnerability, and Adaptive capacity (Weber, Sadoff, Zell, & Sherbinin, 2015). These indicators are expected to help local governments develop targeted adaptation policies for various locations, based on spatial and socio-economic vulnerability and exposure. These studies consider urban-heat-island (UHI) mapping to be an essential component of their methodologies.

Several studies are investigating UHI-mapping globally, as well as in India. However, very few studies have investigated the association between temperature and mortality in Indian cities. Azhar et al. (2014) estimated excess mortality in Ahmedabad during the 2010 heatwave (Azhar, et al., 2014). Mazdiyasni et al. (2017) estimated the impact of heat-related mortality in India, concluding that there were 'statistically significant increases in heatwaves corresponding to a 146% increase in the probability of heat-related mortality events of at least 100 people or more' (Mazdiyasni, et al., 2017). Heat-related mortality is projected to double in Indian cities by 2080 (Dholakia, Mishra, & Garg, 2015).

These studies generally consider the ambient temperature when attempting to determine health impacts. Studies reveal that there are too few monitoring stations, leading to insufficient capturing of 'top-oclimatic and biophysical variations' (Oyler, Dobrowski, Holden, & Running, 2016), especially in developing and low-income countries (Colombi, De Michele, Pepe, & Rampini, 2007; Vancutsem, Ceccato, Dinku, & Connor, 2010). Acknowledging the role that air temperature plays in climatological modelling, these studies propose to assess satellite-based Land Surface Temperature (LST), instead of interpolation (Mostovoy, King, Raja Reddy, Kakani, & Filippova, 2006).

3. Methodology

The scope of this study has been restricted to areas that fall under the jurisdiction of the Ahmedabad Municipal Corporation (AMC). Ahmedabad is the largest city in the state of Gujarat, India. It recently became the first Indian city to be recognised as a 'World Heritage City' by UNESCO. It is located on the banks of the Sabarmati River, almost 80 km away from the Gulf of Khambhat on the Arabian Sea. The city falls within the hot and dry climate zone (ECBC, 2007). Based on Census 2011 data, Ahmedabad was promoted to a Tier-X city (as defined by the sixth central pay commission) in 2015 (MoF, 2015). It is the fifth-most populous city in India, housing 5.5 million people, as per the 2011 Census; this number has now risen to almost 7.8 million people (Tsuboi, 2019). Fig. 1 shows the location of Ahmedabad on the map of India, alongside an AMC ward map.

3.1. Data

Four datasets have been used for this study of Ahmedabad: 1) daily mortality data, 2) daily air-temperature data, 3) daily land-surface-temperature data and 4) land-use data.

3.1.1. Daily mortality data

Daily all-cause mortality data, at the individual level, have been collected for the years 2001 to 2015 from the office of the Registrar of

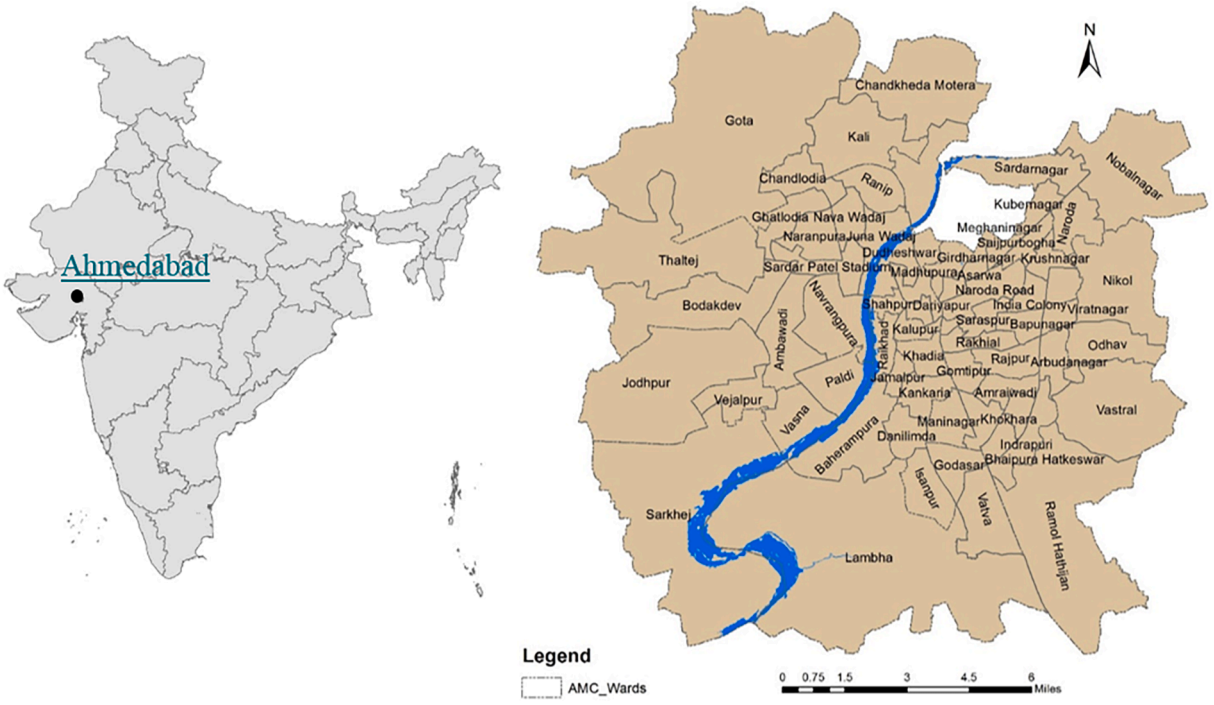

Fig. 1. Location and Ward Map of the Ahmedabad Municipal Corporation Area.

Births, Deaths, and Marriages, Ahmedabad Municipal Corporation (AMC). The data comprises of the registration numbers and names of deceased people, their dates of death and registration, and their age, gender, and residential addresses. A total of 554,553 (2001–2015) data points form the dataset, which documents 7–8 deaths per 1000 people per year, indicating a close match with the crude death rate in Ahmedabad district (GSIDS, GoG, 2016). The cremation or burial of a deceased person requires registration of death and a death certificate in Ahmedabad (Hess, et al., 2018). The data available in the local language (Gujarati) have been cleaned and translated into English for further use. Table 1 presents monthly mortality data across the whole 15-year period.

The data have been aggregated for analysis at the level of daily total mortality in the city, using air-temperature values. For the analysis of land-surface-temperature data, the daily mortality values have been aggregated for each of the 64 wards. This has been done by mapping residential addresses from the dataset to urban wards, using a customised 'lookup' algorithm in Visual Basic-Microsoft Excel 2013©. Less than 5% of the data points had addresses that fell outside the AMC jurisdiction; these have been removed from the final dataset.

3.1.2. Daily Air-Temperature data

Historical daily-maximum temperature and minimum temperature data for the 2001–2015 period have been extracted for relevant grid locations and timeframes from gridded data available from the Indian Meteorological Department, as used by Mukherjee & Mishra (2018). The latter study observed daily temperature data for the 1951–2013 period, as prepared by Pai (2014). This dataset was developed using inverse distance-weighted (IDW) interpolation at 0.25° × 0.25° spatial resolution from observations recorded by 6995 stations across India. As Ahmedabad falls across 4 data grids, as shown in Fig. 2, a weighted average value, based on urban areas that fall within each of the four

Table 1
Month-wise Total All-cause Mortality in Ahmedabad between 2001 and 2015.

	Jan	Feb	Mar	Apr	May	Jun	Jul	Aug	Sep	Oct	Nov	Dec	Total
2001	3368	2213	2306	2383	2426	1961	2314	2823	2465	2355	2457	2442	29,513
2002	2448	2413	2382	2146	2438	2276	2233	2402	2415	2513	2527	2565	28,758
2003	2633	2271	2559	2731	3043	2313	2371	2760	2689	2946	2526	2725	31,567
2004	2776	2471	2807	2463	2567	2263	2270	2782	2637	2555	2755	2664	31,010
2005	2936	2490	2392	2543	2759	2448	2507	2679	2683	2762	2991	3148	32,338
2006	3028	2571	2711	2542	2853	2598	2655	3672	4688*	3730	2962	2984	36,994
2007	3042	2461	2649	2800	2910	2771	2941	2880	2954	3197	3052	3122	34,779
2008	3422	3431	2999	3091	2940	2566	2707	3132	2948	3020	3125	3014	36,395
2009	3284	2801	3066	3132	3166	2791	3033	3223	2948	3092	3040	3354	36,930
2010	3581	2810	3064	3282	4497*	2970	2662	3385	3468	3226	3071	3682	39,698
2011	3985	2945	3174	3176	3095	2988	2915	3715	3471	3752	3264	3452	39,932
2012	3936	3422	3541	3211	3417	2986	3037	3347	3650	3604	3732	3563	41,446
2013	4008	3370	3717	3428	3862	3238	3672	3905	3757	3641	3831	3884	44,313
2014	4217	3468	3758	3902	4316	3858	3341	3977	3864	4015	3754	4064	46,534
2015	4109	3949	3821	3444	4011	3393	3394	3422	3658	3754	3679	3712	44,346
Average	3385	2872	2996	2952	3129	2761	2803	3207	3115	3211	3118	3225	36,970

*September 2006 – the peak of the chikungunya epidemic – 1,448 additional deaths in September 2006 (Mavalankar, Shastri, Bandyopadhyay, Parmar, & Ramani, 2008); May 2010 – an additional 1,344 all-cause deaths during the May 2010 heatwave (Azhar, et al., 2014).
Source: AMC.

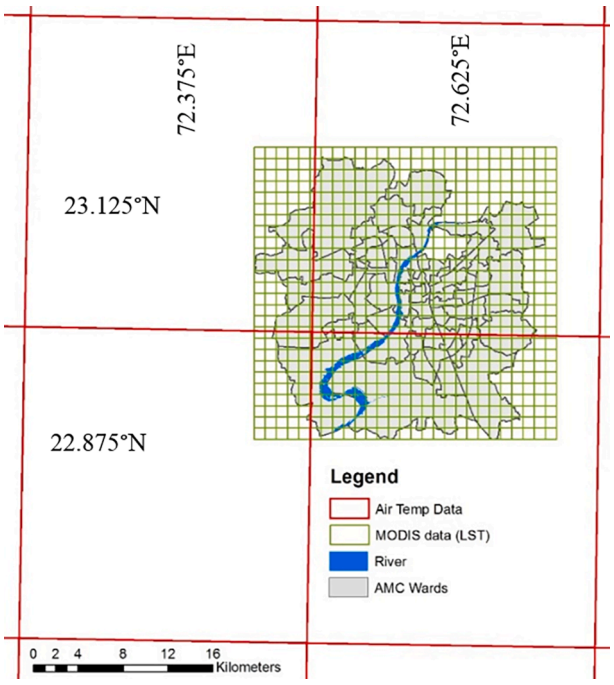

Fig. 2. Map of Ahmedabad Showing Data Resolution for Air- and Land-Surface Temperatures.

grids, has been used to arrive at the daily air-temperature (AT) values. The monthly average of daily mean temperatures between 2001 and 2015 is shown in Fig. 3.

3.1.3. Daily land-surface temperature

Daily land-surface temperature (LST) data from 2001 to 2015 (for both daytime and nighttime) have been extracted from satellite images for this study. Daytime as well as nighttime Moderate Resolution Imaging Spectroradiometer (MODIS) data, generated by the NASA satellite Terra, have been collected from the US Geological Survey (USGS)'s Land Processes Distributed Active Archive Center (LP DAAC) website (https://lpdaac.usgs.gov/), due to missing data from the Aqua satellite. MODIS Land Surface Temperature and Emissivity (MOD11), specifically MOD11A1 Version 6 from Terra, provides daily 1 km × 1 km pixel-size data. This is a processed-image product with updated regression algorithms that are sensitive to cloud contamination and minor adjustments in classification-based surface-emissivity values, especially for the bare-soil and rocks land-cover types, day/night adjustment for improved results in desert regions, and related data. It provides land-surface-temperature data for around 990 pixels for Ahmedabad city, in comparison to only 4 grids of air-temperature data, making it possible to analyse mortality in relation to urban micro-climates. These data have been validated using *in situ* measurements; the standard deviation of validation errors has been shown to be less than 0.5°K for 12 validation datasets (Wan, 2014).

These images have been further processed using ArcPy, a python site package for ArcGIS 10.5.1 software scripting, to extract temperature values from the pixel's digital number (DN) values. As these were in °K format, they had to be converted into °C. The following formula was used to process them:

$$LST\ (^{\circ}C) = (Raster\ Image(DNvalue)*0.02\ ) - 273.15 \quad (1)$$

990 daily pixel values for Ahmedabad between 1/1/2001 and 31/12/2015 for daytime and nighttime data were processed to generate LST values across 64 wards in Ahmedabad. These pixels were further clubbed at ward level to arrive at the daily ward-level LST values. Fig. 4 presents a sample of LST values for one summer day (25 May 2015) and one winter day (25 December 2015).

3.1.4. Land-use data

The land-use composition of each ward within the AMC was extracted by processing Landsat images from the United States Geological Survey (USGS) Earth Explorer – Global Land Survey (GLS) – for the years 2000, 2010, and 2017. A hybrid classification approach was adopted, using ENVI 5.3, and ArcGIS 10.5.1 software packages. The 30-meter by 30-meter land-use resolution images were classified into 6 groups: built-up area, land under agriculture, green spaces, open areas, river, and water bodies (Garg et al., 2018) (Fig. 5).

3.1.5. Modelling

As a general rule, mortality has been found to be lowest at average temperatures and higher at below- and above-average temperatures (Armstrong, 2006). Thus, ordinary least squares and log-linear functions are not sufficient. For the purposes of this study, we considered the widely cited method proposed by (Gasparrini, Armstrong, & Kenward, 2010) for establishing the effect of temperature on overall mortality. In this approach, the main unit of analysis is the day, not the person. This approach models changes in the day-to-day variation in the number of deaths, as a consequence of changes in temperature, for a given population. Thus, this approach makes it possible to assess whether short-term variations in temperature have led to variations in health outcomes. Ideally, researchers prefer to associate variations in cause-

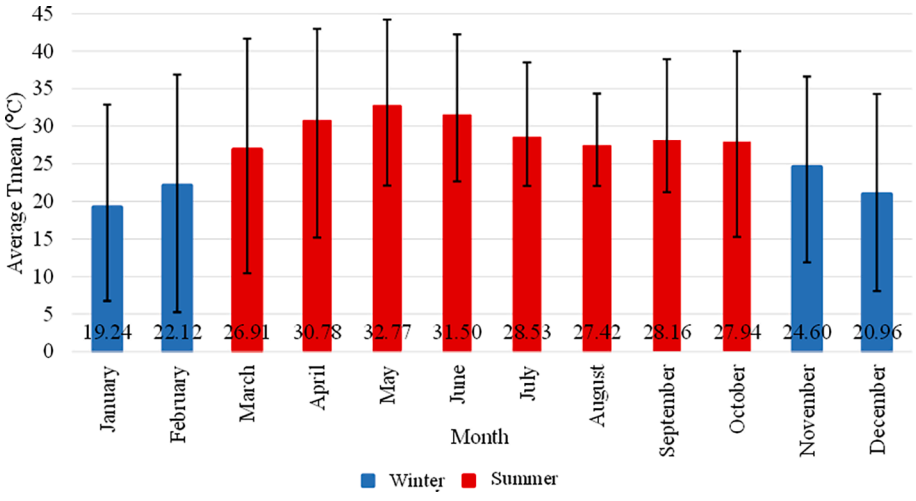

Fig. 3. Month-wise Average Daily Mean Temperature across 2001–2015 for Ahmedabad.

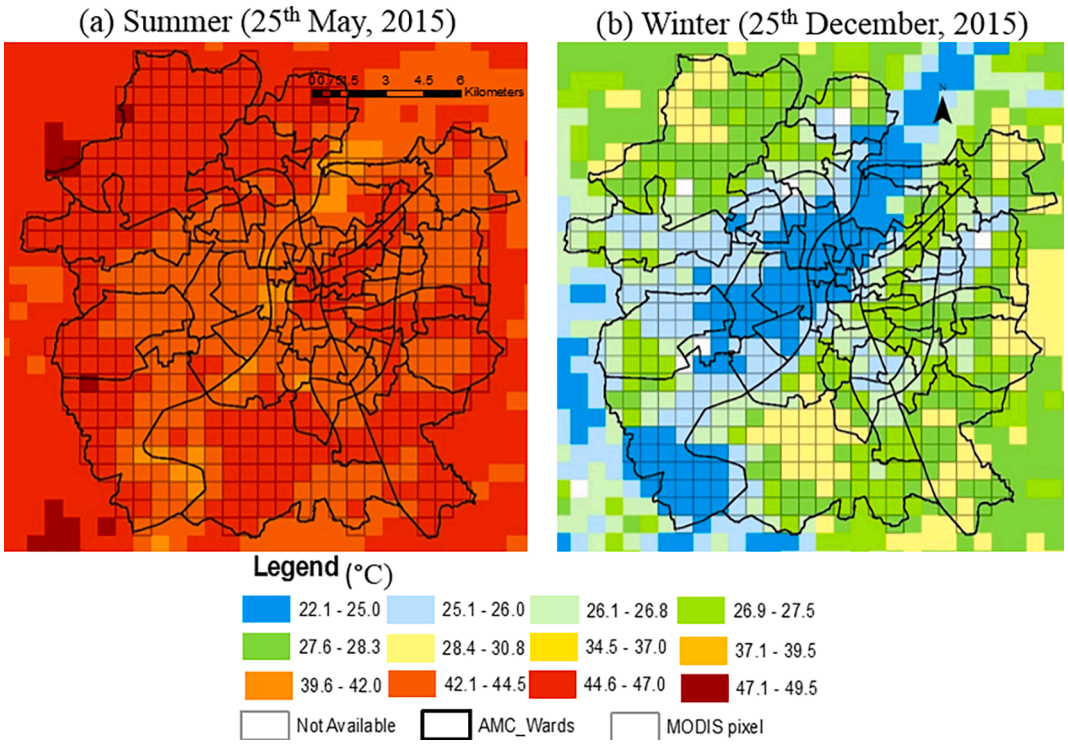

Fig. 4. Land Surface Temperature for Ahmedabad City.

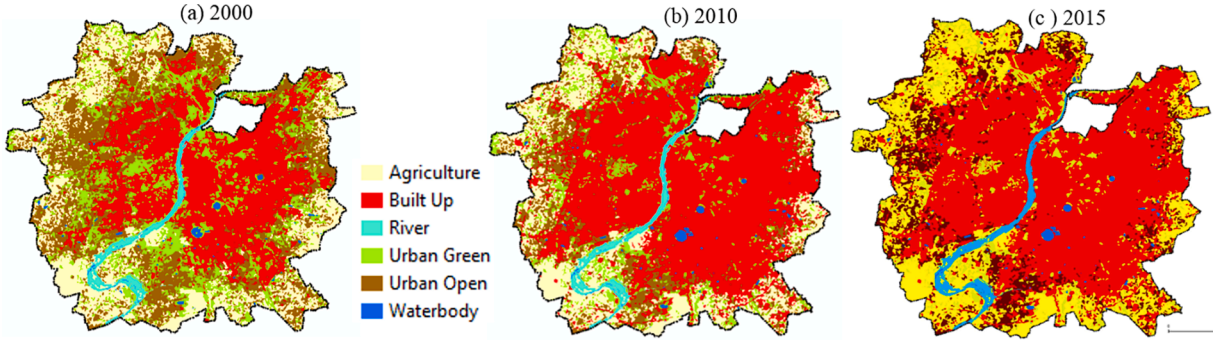

Fig. 5. Land-use maps for Ahmedabad city for the years 2000, 2010, and 2015.

specific and age-specific mortality with temperature. However, information on the cause of mortality is rarely available. Under these circumstances, all-cause mortality provides good insights into the health impacts of temperature changes. For this reason, studies of all-cause mortality and temperature have been carried out around the world.

The relationship between temperature and mortality is expressed as 'U', 'V', or 'J' shaped. Researchers have modelled temperature as smooth curves, using spline functions (Armstrong, 2006). Gasparrini et al. (2010) have suggested a distributed-lag non-linear-modelling (DLNM) approach, which allows assumptions about variable relationships to be relaxed, in contrast to a linear modelling approach. DLNM allows the 'effects to vary simultaneously both along the space of the predictor and in the lag dimension of its occurrence' (Gasparrini, Armstrong, & Kenward, 2010). The non-linearity here comes from modelling the relationship between temperature and mortality as a natural cubic-spline function, while the distributed lag captures the 'delayed effects' of any exposure event (exposure to temperature in this study) in terms of time-delay (days in this study). A spline function is devised by joining polynomials at fixed points. The points at which these functions join are called knots. A cubic spline is a spline function formed by joining third-order polynomials. Hence, the cubic spline and natural cubic-spline functions aid the construction of smooth curves. For this reason, the exposure–response curves generated here with a natural cubic-spline function show smooth curves.

The literature on the relationship between temperature and mortality discusses the role of seasonality in such assessments (Parks, Bennett, Foreman, Toumi, & Ezzati, 2018; Gasparrini, et al., 2015). For this reason, we have further refined the temperature inputs, based on seasonality. The summer season in Ahmedabad is considered to last from 1 March to 31 October each year; this time span is used to understand the effect of heat and extreme-heat situations, using maximum air temperature (AT_{max}) and daytime LST (LST_{day}) for similar months. It is worth noting here that there are spells of rain from June to September, which may subdue temperatures. However, the average AT_{max} temperatures during 2001–2015 in July, August, September, and October were 32.2 °C, 30.9 °C, 32.8 °C, and 35.2 °C, respectively. To comprehend cold and extreme cold, a winter season lasting from 1 November to 28/29 February was considered; both minimum air temperature (AT_{min}) and nighttime LST (LST_{night}) were used. A similar seasonal delineation was used by (Dholakia, 2014) to estimate the relationship between temperature and mortality in Indian cities. The Quasi Akaike Information Criterion (QAIC) shows improvements over T_{mean} models for AT and LST.

The relationship between temperature and mortality is generally described in terms of the 'relative risk' (RR) of mortality as the temperature changes. The relativity here comes from comparing the risk of mortality at any given temperature value to the risk of mortality at a baseline temperature value (or centring temperature value) (Chen, Xiao, Zhao, & Zhang, 2017; Guo, Barnett, Pan, Yu, & Tong, 2011). At the centring temperature value, the risk of mortality is taken as 1. Thus, the relative risk of mortality at any given temperature can be computed in reference to the baseline/centring temperature value of 1.

RR is generally calculated with reference to a baseline/centring temperature, at which the risk of mortality is minimal (Tobías, Armstrong, & Gasparrini, 2017). The minimum mortality temperature (MMT) reflects the most comfortable, optimum temperature. The MMT varies from place to place and mortality rates increase at temperatures that are lower or higher than the local MMT (Yin, Wang, Ren, Li, & Guo, 2019). Generally, this minimum mortality temperature (MMT) is used as the centring (baseline) temperature when comparing data across cities (Curriero, et al., 2002). Since, the RR thus computed refers to the MMT of a particular city, city-specific characteristics must be captured appropriately. In this way, the results for each individual city are rendered comparable. Thus, the approach adopted in the present study, of using MMT as the centring/baseline temperature, is also applicable to multi-city studies.

However, this may not hold true for intra-city comparisons of RR. The temperature and locational characteristics of a city that influence its climate are common for intra-city units (e.g. wards). This study aims to understand the influence of land use (reflected through LST) on mortality (at intra-city level) and also to compare the association between air temperature and mortality with the association between land-surface temperature and mortality. For the purposes of this study, therefore, we have not used the MMT value as the centring value.

The literature suggests a close co-relationship between air temperature and LST. Several papers have proposed the use of regression-based statistical approaches, the temperature-vegetation index, and physical approaches using energy balance to estimate air temperature from LST (Hadria, et al., 2018; Benali, Carvalho, Nunes, Carvalhais, & Santos, 2012; Gallo, Hale, Tarpley, & Yu, 2011; Mostovoy, King, Reddy, Kakani, & Filippova, 2006; Cresswell, Morse, Thomson, & Connor, 1999). In this study, a simple regression of daily air and land-surface temperatures was applied to 15 years' worth of data to establish a relationship between air temperature and LST, in order to determine an appropriate centring value for RR assessments.

The regression results for the $AT_{max} - LST_{day}$ relation, using summer temperatures during the 15-year period of 2001–2015, suggest that there is a 1:1 relation between the two temperature values for Ahmedabad at 33 °C. Thus, the RR values computed here refer to 33.50 °C. For the cold-mortality relationship assessment, the AT and LST of Ahmedabad have a linear relationship and do not indicate a convergence point. For this reason, an AT value corresponding to the 50th percentile of LST (15.36 °C) has been used as the centring temperature for RR computations of cold-mortality relations (Refer Supplementary Material).

Equation (2) describes the statistical form of the generalised additive-model framework used for this assessment. DLNM structures depend on 'cross-basis' functions, as described by Gaspirrini (2010). The dependent variable estimates for exposure are the sum of products of the basis functions for exposure and lag, referred to as 'cross-basis' functions (Neophytou, et al., 2018).

The dependent variable for this exercise was the daily total all-cause number of deaths reported across Ahmedabad (count data) between 2001 and 2015. The independent variables were the daily maximum/minimum air temperature data – AT_{max} and AT_{min} (for summer/winter assessments) for Ahmedabad city, while time and day of the week (DOW) were indicator variables.

$$Log[E(Y_i)] = \sum f(x_{i,b}) + g(t_i) + DOW + \varepsilon \quad (2)$$

where, $x_{i,b} = s(AT_i)$

Where Y_i is the daily number of deaths on i^{th} day and $E(Y_i)$ is the expected daily number of deaths on i^{th} day. Since mortality provides the count data, the model assumes that it will follow a Poisson distribution with over-dispersion; $s(AT_i)$ is a cross-basis function (refer to Gasparrini et al. (2010) for a definition and description of cross-basis functions) that represents the bi-dimensional space of functions, simultaneously describing the shape of the relationship of independent variables ATmax and ATmin, respectively, for each day *i* and its distributed-lag effects. Since the algebraic concept of a DLNM is quite complex, involving three-dimensional arrays (Gasparrini, Armstrong, & Kenward, 2010), the cross-basis function is described in a simplified manner as $x_{i,b}$, where *b* represents degrees of freedom. Function *f* is a smoothened representation using natural cubic splines for $x_{i,b}$. Time (t), in terms of each day *i*, is also represented through a natural cubic-spline smoothened function g (t_i). DOW is the categorical variable representing the day of the week for each day *i*. The day-of-the-week variable works as a control parameter here, since there have been observed variations in the population's exposure to temperature on weekdays versus the weekend. Although this could have been a binary variable, indicating weekday/non-weekday, there have been concerns about the definition of 'weekend' as a 'day off work'. This definition varies across sectors and countries. It should be noted here that DOW is a simple representation of factors that determine exposure to temperature. Daily commute/travel time, travel distance, mode of transport, and a number of similar urban-transport factors have also been considered recently (Yang, Hu, & Wang, 2019). DOW has been included in the present study to ensure comparability of results internationally, including with other studies using similar methods (Lee, et al., 2018; Gasparrini & Leone, 2014; Gasparrini, Armstrong, & Kenward, 2010).

All-cause mortality data between 2001 and 2015, aggregated at the ward level, is used as the dependent variable for LST-based estimations. Like the AT model, the independent variables include the daily ward-level average day/night LST-, LST_{day}, and LST_{night} (for summer/winter assessment) for Ahmedabad city, with time and day of the week (DOW) as indicator variables. Since the ward-level average LST is expected to reflect the underlying land-use pattern, variables representing land-use parameters have not been included. However, a categorical variable representing wards has been introduced into Equation (2). Equation (3) describes the statistical form in the generalised additive-model framework:

$$Log\left[E\left(Y_{ij}\right)\right] = f(x_{ij}) + g(t_i) + Ward_j + DOW + \varepsilon \quad (3)$$

where Y_{ij} is the daily number of deaths on the i^{th} day in the j^{th} ward. Since mortality is count data, the model assumes that it follows a Poisson distribution with over-dispersion. The LST for each day *i* and ward *j* and time in terms of each day *i* are represented by x_{ij} and t_i, respectively, through natural cubic-spline-based smoothening functions *f* and *g*. DOW is the categorical variable representing the day of the week for each day *i*.

To model the effects of temperature, the literature suggests that the natural cubic-spline function at three degrees of freedom should be used for smoothening, since it enables researchers to capture short-term effects and to exclude the impact of long-term and seasonal trends (Dholakia, 2014; Rocklov, Barnett, & Woodward, 2012; Hajat, Kovats, & Lachowycz, 2007). These long-term and seasonal trends have been captured using time as a control variable (t_i) with 7 degrees of freedom per year.

The next step in the process is the computation of the attributable factor (AF) – the excess fraction attributable to temperature. AF is defined as the percentage share of mortality that 'would not have occurred in the absence of exposure either among the exposed population or among the total population' (Steenland & Armstrong, 2006). The AF for heat-related mortality and cold-related mortality in Ahmedabad have been calculated using the method proposed by (Gasparrini &

Leone, 2014), who suggested two approaches: a forward approach to assess the future mortality burden; and a backward approach to assess the current mortality burden, based on a given exposure event. Each backward AF for time T compares the association with observed temperatures in the past L days to a constant exposure x_0. According to Gasparrini & Leone (2014), the backward AF provides more accurate estimators through the regression model, where distributed-lag terms at times $t-\ell$ contribute to the risk at time t (Gasparrini & Leone, 2014). They describe the equation for AF estimation as follows:

$$AF_x = 1 - \exp(-\beta x) \quad (4)$$

here, βx is the relative risk associated with the exposure. For a given exposure x, β_x is the risk associated with the exposure; it usually corresponds to the logarithm of a ratio measure such as relative risk, relative rate, or odds ratio (Gasparrini & Leone, 2014)

4. Results and discussion

The dependent variable was tested for spatial correlation. The Moran's I values indicated no correlation. The model residuals were also tested for spatial autocorrelation calculations, and a cross correlogram was generated in R, using the package, ncf v1.2–6. An exploratory analysis for time-lag (in days) values ranging from 0 to 30 was carried out for both summer and winter datasets related to AT and LST mortality relations. An inspection of the results and plots (Refer Supplementary Material) revealed that the association between temperature and mortality persisted across the lag period of 0 to 5 days. However, the effect size (reflected through RR) was observed to decrease with increasing lag. Thus, lag with maximum RR, which represents the highest effect size, was selected here to represent the association between temperature and mortality. Thus, a lag of 0 for AT_{max} (summer air temperatures) and a lag of 2 (winter air temperatures) were considered for the AT_{min} analysis. Similarly, a lag of 2 for LST_{day} (summer temperatures) and LST_{night} (winter temperatures) was used for the LST analysis in the model. It should be noted here that several studies have shown that increased heat has an immediate impact on mortality, especially in extreme-heat situations, in contrast to reduced heat (winter temperatures). Rocklov & Forsberg (2008) and Yang et al. (2019) found that the effect size of summer temperatures was most significant on the current day (lag = 0) (Rocklov & Forsberg, 2008; Yang, et al., 2019).

Fig. 6 (a), (b), (c), and (d) show the centring temperature (CT), temperatures at the 5th, 50th, and 95th percentiles (dashed lines), RR, and RR values at a 95% confidence interval (dotted lines in red and blue) for heat-mortality and cold-mortality assessment, using AT and LST respectively. The RR values have been calculated in reference to 33 °C for the summer temperature-based analysis. For the cold-mortality relationship assessment, the 50th percentile temperature of LST (15.36 °C) has been used to centre the RR computation.

Across both models of air temperature-related mortality (AT_{max} and AT_{min}), the relationship is found to be significant at 95% confidence. Fig. 6 (a) and (b) show that air temperature and mortality associations for summer (AT_{max}) and winter (AT_{min}) indicate a 'J'/'hockey-stick' curve. This smooth curve is due to the parameters being modelled as natural cubic-spline functions, as discussed in Section 3.1.5 Modelling. The dotted lines indicate the 95% confidence interval level of RR across temperature ranges. The dashed lines indicate the 1st, 5th, 50th, 95th, and 99th percentile temperature levels for AT_{max}, AT_{min}, LST_{day}, and LST_{night} in Fig. 6 (a), (b), (c) and 6 (d), respectively. For the summer-maximum-temperature (AT_{max}) association, as the temperature rises beyond the 95th percentile AT_{max}, the RR values increase at a higher rate. At the 99th percentile temperature of 44 °C, the RR is 1.64 (Table 2), while at 47 °C it crosses the RR of 2. Similarly, for the winter T_{min} temperature at the 1st percentile temperature of 8.84 °C, the RR is 1.68 while, at 3 °C, the RR crosses 2. The attributable fractions for AT-mortality associations are 5.80% and 3.17% for heat and cold, respectively.

Fig. 6 (c) and (d) indicate that, like AT, LST and morality associations for summer and winter also form a 'J'/'hockey-stick' curve because they are also modelled as a natural cubic spline. For the summer-maximum-temperature (T_{max}) association represented by summer day LST, as the temperature rises beyond the 50th percentile LST_{day}, i.e. 41.20 °C, the RR values show an increasing slope. However, beyond the 95th percentile LST_{day} of 48.3 °C, the curve begins to flatten; the RR is 1.21 at the 95th percentile LST_{day} and 1.27 at 52.7 °C, the 99th percentile

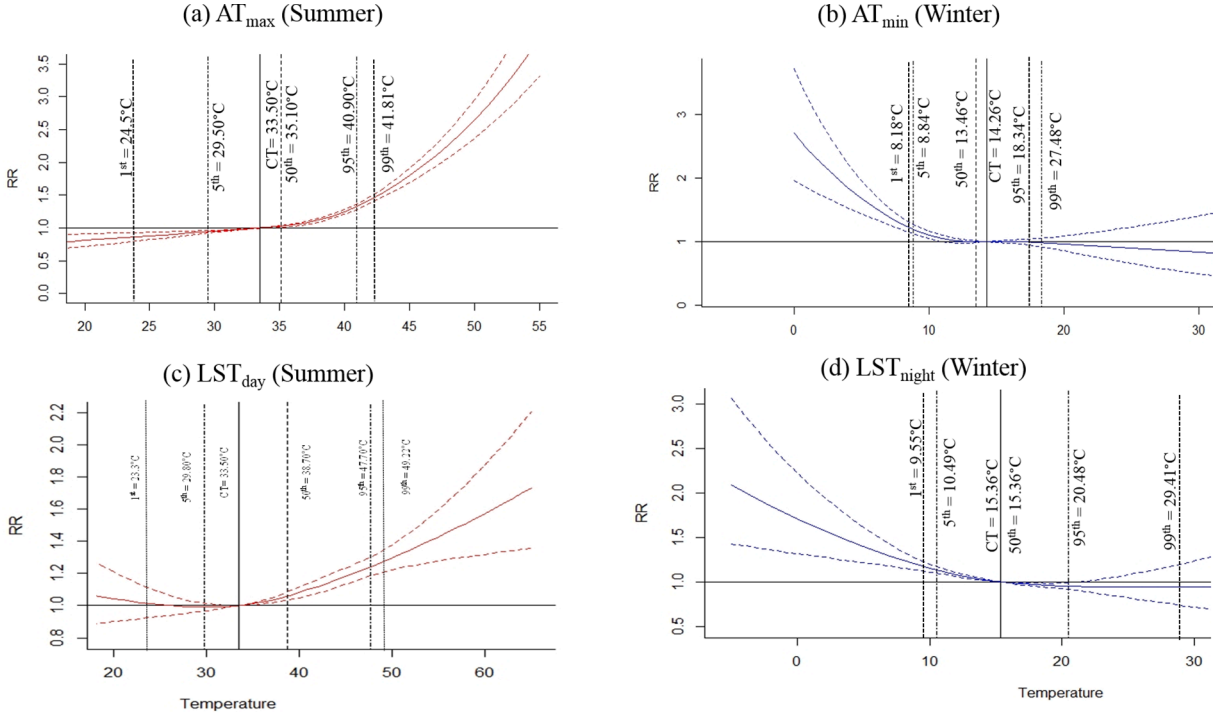

Fig. 6. Temperature and Mortality Risks in Ahmedabad.

Table 2
RR and AF for AT-mortality Association in Ahmedabad.

	Summer (AT) Maximum	Summer (LST) Daytime	Winter (AT) Minimum	Winter (LST) Night time
RR at temp 1 percentile	0.90	0.85	1.68	1.29
RR at temp 5 percentile	0.93	0.97	1.18	1.15
RR at temp 50 percentile	1.02	1.12	0.999	1.00
RR at temp 95 percentile	1.32	1.21	0.98	0.95
RR at temp 99 percentile	1.66	1.27	0.93	0.94
AF-backward	5.80%	7.29%	3.17%	1.50%

LST_{day} (Table 2). Similarly, for the winter assessment using LST_{night}, the slope starts to grow steeper after the 5th percentile LST_{night} of 10.96 °C, with RR of 1.15, leading to the 1st percentile LST_{night} – 7.4 °C RR of 1.29. The AF, as computed for LST_{day} summer and LST_{night} winter temperatures, is 7.29% and 1.50% respectively.

A comparison of the AF estimates for AT_{max} and LST_{day} mortality associations during summer (March–July) in Ahmedabad points to a 17.40% underestimation using AT. The LST_{day} recorded for 1 March–31 December between 2001 and 2015 is, on average, 2.02 °C higher than the AT_{max}. Similarly, the AT_{min} and LST_{night} estimates indicate an overestimation in the comparison of AF values. The LST values are derived from satellite data, based on two overpasses a day. Both the daytime and nighttime LST data used here come from the Terra satellite, as the Aqua satellite has too much missing data. It must be noted that the daytime overpass time for Terra is 10:30 AM while the nighttime overpass time is 10:30 PM. However, the AT_{max} for Ahmedabad is generally expected to occur around 3–4 PM. The AT at 3 PM is an average 5 °C higher, and the AT at 4 PM is an average 5.5 °C higher than the AT recorded at 10 AM between 1 March and 31 October (Refer Supplementary Material). Thus, the LST_{day} recorded at 10:30 AM is expected to be lower than the LST_{day} that would have been recorded between 3 and 4 PM. Thus, Terra sensors report a relatively cool daytime LST (Crosson, Al-Hamdan, Hemmings, & Wade, 2012) and the actual underestimation of AF is expected to be even larger than it appears in this study. Again, the AT_{min} is recorded at around 7:00 AM, while the LST_{night} is recorded 9 h earlier, at 10:30 PM. The LST_{night} is, on average, 3.59 °C higher than the AT_{min} recorded at 7 AM the following morning. As there appears to be uncertain evidence of overestimation, there is clearly a need for further investigation. More satellites or improved imagery could improve temperature-related mortality associations made using LST.

To further understand how LST_{day} plays out in temperature-related mortality relations, ward-level LST_{day}-mortality estimates have been calculated individually for each of the 64 wards over 2001–2015. Ward-level land-use data have been used to arrive at the share of built-up spaces for each ward. We observe that wards with a higher share of built-up spaces show higher RR values than those with a higher share of non-built-up spaces within Ahmedabad. No spatial autocorrelation is observed here. To further explore how mortality risks vary across different land-use compositions, a regression analysis for RR with the land-use share of non-built-up (NBU) spaces, has been carried out, using the generalised linear model. RR varies with temperature. Hence, in order to determine the relationship between RR and land use, temperature must be used as a control variable. Here, a regression analysis that controls for three selected temperature values of 35 °C, 40 °C, and 45 °C is shown as an illustration. The R-square value is 0.2585. The p-value for NBU is 0.0635 – significant at 90% confidence levels. In addition, the RR values and land-use shares for each ward at selected temperatures have been mapped, and slopes for the linear relation of RR values to land-use shares have been calculated. As Fig. 7 shows, as the share of built-up

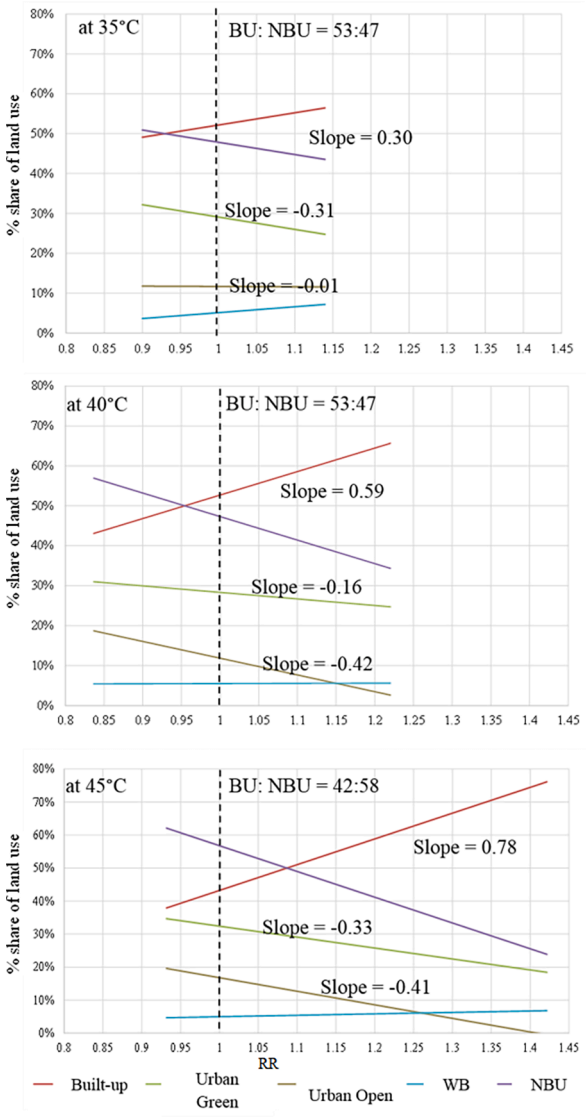

Fig. 7. Land-use Share and RR Relations in Ahmedabad.

spaces increases, the RR also increases. Fig. 7 (a) shows that, at 35 °C LST_{day}, various wards in Ahmedabad experience a range of mortality risks related to temperature, since the localised temperature experienced in the wards varies, based on land use. A similar analysis at 40 °C (Fig. 7 (b)) and 45 °C (Fig. 7 (c)) shows a much steeper slope. All figures show an increase in RR as green and open spaces decrease in the land-use mix. As built-up spaces increase by 1% in the land-use mix, the relative risk of mortality increases by 0.59 points at 40 °C and by 0.78 points at 45 °C. These results also suggest an increase in relative risk of mortality as non-built-up spaces (green, blue, and open spaces) decrease in the land-use mix. For the RR to be 1 at 35 °C, 40 °C, and 45 °C, the average mix of built-up to non-built-up spaces in the city would be 53:47, 53:47, and 42:58 respectively. This demonstrates the need for more non-built-up spaces to prevent the RR from increasing as the temperatures increases. Thus, land-use mix has an impact on the relative risk of mortality – with more built-up spaces increasing mortality risks.

5. Conclusion

Land-use changes play a significant role in determining localised temperatures and urban heat islands in a city. As the climate changes and temperatures rise, the influence of such micro-climatic variations will be exacerbated. This study explores the impact of land use on

temperature in the context of heat-related mortality, using Ahmedabad city as a case study. MODIS images from NASA satellites, temperature data from IMD, and daily all-cause mortality data from the Ahmedabad Municipal Corporation between 2001 and 2015 have been used to carry out distributed-lag non-linear modelling. The inherent land use in the city is reflected through the land-surface temperature, as captured by satellites. When satellite images are processed, we find substantial variations in temperature across the city. This points towards variation in the heat impacts faced by different neighbourhoods within the city, which translates into differential mortality risks faced by people living in different parts of the city.

Land-surface and air temperature are associated with very different mortality risks, indicating that localised temperature variations influence mortality risks. The model results suggest that an urban microclimate, as represented by land-surface temperatures, is a better indicator of relative mortality risk than air temperature. With several cities across India and the globe facing an increased number of concurrent hot days and hot nights, due to the changing climate, it has become essential for city governments to implement policies to prevent heat-related deaths. A few cities, including Ahmedabad, have come up with the 'Heat Action Plan', an early-warning system that includes a list of dos and don'ts for heat-wave situations. From the disaster-management point of view, these are short-term actions that come into play during the 4–5 peak months of summer. Moreover, these action plans do not consider local temperature variations, instead treat the city as a monolith. Cities must take additional long-term actions to prevent heat-related deaths. As built-up spaces increase by 1% in the land-use mix, the relative mortality risk increases by 0.59 points at 40 °C and by 0.78 points at 45 °C. Landscape and land-use planning could prove to be an effective tool, enabling city administrators to create positive change, as part of a long-term effort. Appropriate measures to ensure green and open spaces across the city, such as incorporating plantation activities, green/cool roofs, and mandatory non-built cover maintenance in city-level plans and building regulations, must be considered as an essential part of urban development and public-health policies.

Temperature-exposure-related mortality risks have become a major public-health concern as climate change accelerates. This study reveals the implications of land-use planning for public-health management, providing further evidence of the need for a holistic spatial-planning approach towards building climate-change resilience.

CRediT authorship contribution statement

Vidhee Avashia: Conceptualization, Methodology, Data curation, Software, Writing - original draft, Visualization, Investigation, Writing - review & editing. **Amit Garg:** Conceptualization, Supervision, Validation, Writing - review & editing. **Hem Dholakia:** Methodology.

Declaration of Competing Interest

The authors declare that they have no known competing financial interests or personal relationships that could have appeared to influence the work reported in this paper.

Acknowledgements

This work has been partly supported by the National Network Programme on Climate Change and Human Health under Climate Change Programme by the Department of Science and Technology, Ministry of Science and Technology, Government of India, under the project titled "Impact of Heat Extremes on Health in Urban India under a Changing Climate" (DST/CCP/NHH/101/2017) and European Union's Horizon 2020 research and innovation programme under grant agreement 821471 (ENGAGE).

Appendix A. Supplementary data

Supplementary data to this article can be found online at https://doi.org/10.1016/j.landurbplan.2021.104107.

References

Anderson, B., & Bell, M. (2009). Weather-related mortality: How heat, cold, and heat waves affect mortality in the United States. *Epidemiology, 20*(2), 205–213.

Armstrong, B. (2006). Models for the relationship between ambient temperature and daily mortality. *Epidemiology, 17*(6), 624–631. https://doi.org/10.1097/01.ede.0000239732.50999.8f.

Azhar, G. S., Mavalankar, D., Nori-Sarma, A., Rajiva, A., Dutta, P., Jaiswal, A., Sheffield, P., Knowlton, K., Hess, J. J., & Akiba, S. (2014). Heat-related mortality in India: excess all-cause mortality associated with the 2010 Ahmedabad heat wave. *PLoS ONE, 9*(3), e91831. https://doi.org/10.1371/journal.pone.0091831.

Basu, R., & Ostro, B. (2008). A multicounty analysis identifying the populations vulnerable to mortality associated with high ambient temperature in California. *American Journal of Epidemiology, 168*(6), 632–637. https://doi.org/10.1093/aje/kwn170.

Basu, R., & Samet, J. (2002). Relation between elevated ambient temperature and mortality: A Review of the epidemiologic evidence. *Epidemiologic Reviews, 24*(2), 190–202. https://doi.org/10.1093/epirev/mxf007.

Benali, A., Carvalho, A., Nunes, J., Carvalhais, N., & Santos, A. (2012). Estimating air surface temperature in Portugal using MODIS LST data. *Remote Sensing of Environment, 124*, 108–121. https://doi.org/10.1016/j.rse.2012.04.024.

Bennett, J. E., Blangiardo, M., Fecht, D., Elliott, P., & Ezzati, M. (2014). Vulnerability to the mortality effects of warm temperature in the districts of England and Wales. *Nature Climate Change, 4*(4), 269–273. https://doi.org/10.1038/nclimate2123.

Brown, R. D., Vanos, J., Kenny, N., & Lenzholzer, S. (2015). Designing urban parks that ameliorate the effects of climate change. *Landscape and Urban Planning, 138*, 118–131. https://doi.org/10.1016/j.landurbplan.2015.02.006.

Chaturvedi, R., Joshi, J., Jayaraman, M., Bala, G., & Ravindranath, N. (2012). Multi-model climate change projections for India under representative concentration pathways. *Current Science, 103*(7), 791–802.

Chen, T.-H., Xiao, L., Zhao, J., & Zhang, K. (2017). Impacts of cold weather on all-cause and cause-specific mortality in Texas, 1990–2011. *Environmental Pollution, 225*, 244–251. https://doi.org/10.1016/j.envpol.2017.03.022.

Colombi, A., De Michele, C., Pepe, M., & Rampini, A. (2007). Estimation of daily mean air temperature from MODIS LST in Alpine areas. *EARSeL eProceedings, 6*(1), 38–46.

Cresswell, M., Morse, A., Thomson, M., & Connor, S. (1999). Estimating surface air temperatures, from Meteosat land surface temperatures, using an empirical solar zenith angle model. *International Journal of Remote Sensing, 20*(6), 1125–1132. https://doi.org/10.1080/014311699212885.

Crosson, W. L., Al-Hamdan, M. Z., Hemmings, S. N. J., & Wade, G. M. (2012). A daily merged MODIS Aqua-Terra land surface temperature data set for the conterminous United States. *Remote Sensing of Environment, 119*, 315–324.

Curriero, F., Heiner, K., Samet, J., Zeger, S., Strug, L., & Patz, J. (2002). Temperature and mortality in 11 cities of the eastern United States. *American Journal of Epidemiology, 155*(1), 80–87. https://doi.org/10.1093/aje/155.1.80.

Dholakia, H. H. (2014). *Climate change, air pollution and public health in India: Impact assessment and adaptation strategies (Doctoral dissertation)*. Ahmedabad, India: Indian Institute of Management Ahmedabad.

Dholakia, H. H., Mishra, V., & Garg, A. (2015). *Predicted Increases in Heat related Mortality under Climate Change in Urban India*. Ahmedabad: Research and Publications, Indian Institute of Management, Ahmedabad (IIMA). Retrieved July 18, 2015, from http://www.iimahd.ernet.in/assets/snippets/workingpaperpdf/14404236732015-05-02.pdf.

Dugord, P.-A., Lauf, S., Schuster, C., & Kleinschmit, B. (2014). November). Land use patterns, temprature distribution, and potential heat stress risk-The case study Berlin, Germany. *Computers, Environment and Urban Systems, 48*, 86–98. https://doi.org/10.1016/j.compenvurbsys.2014.07.005.

ECBC. (2007). Energy Conservation Building Code. New Delhi: Bureau of Energy Efficiency, Ministry of Power, Government of India.

Gallo, K., Hale, R., Tarpley, D., & Yu, Y. (2011). Evaluation of the relationship between air and land surface temperature under clear- and cloudy-sky conditions. *American Meteorological Society, 767*, 775. https://doi.org/10.1175/2010JAMC2460.1.

Garg, A., Avashia, V., & Parihar, S. (2018). *Land use change trends of Indian Cities: A bird's-eye view - vulnerabilities of unplanned urban growth*. New Delhi: SAGE Publications India Pvt Ltd.

Gasparrini, A., & Leone, M. (2014). Attributable risk from distributed lag models. Retrieved from www.biomedcentral.com/1471-2288/14/55. *BMCMedical Research Methodology, 14*(55)

Gasparrini, A., Armstrong, B., & Kenward, M. (2010). Distributed lag non-linear models. *Statistics in Medicine, 29*(21), 2224–2234. https://doi.org/10.1002/sim.3940].

Gasparrini, A., Guo, Y., Hashizume, M., Kinney, P. L., Petkova, E. P., Lavigne, E., … Armstrong, B. G. (2015). Temporal variation in heat-mortality associations: A multicountry study. *Environmental Health Perspectives, 123*(11), 1200–1207. https://doi.org/10.1289/ehp.1409070.

Gover, M. (1938). Mortality during periods of excessive temperature. *Public Health Reports, 53*(27), 1122–1143. https://doi.org/10.2307/4582590.

GSIDS, GoG. (2016). District Human Development Report Ahmedabad. Gandhinagar: Gujarat Social Infrastructure Development Society, General Administration Department (Planning), Government of Gujarat. Retrieved from http://www.in.

undp.org/content/dam/india/docs/human-development/District%20HDRs/9.%20Ahmedabad_DHDR_2016.pdf.
Guo, Y., Barnett, A., Pan, X., Yu, W., & Tong, S. (2011). The impact of temperature on mortality in Tianjin, China: A case-crossover design with a distributed lag nonlinear model. *Environmental Health Perspectives, 119*(12), 1719–1725. https://doi.org/10.1289/ehp.1103598.
Hadria, R., Benabdelouahab, T., Mahyou, H., Balaghi, R., Bydekerke, L., El Hairech, T., & Ceccato, P. (2018). Relationships between the three components of air temperature and remotely sensed land surface temperature of agricultural areas in Morocco. *International Journal of Remote Sensing, 39*(2), 356–373. https://doi.org/10.1080/01431161.2017.1385108.
Hajat, S., Kovats, R., & Lachowycz, K. (2007). February). Heat-related and cold-related deaths in England and Wales: Who is at risk? *Occupational and Environmental Medicine, 64*(2), 93–100. https://doi.org/10.1136/oem.2006.029017.
Hess, J. J., LM, S., Knowlton, K., Saha, S., Dutta, P., Ganguly, P., … Mavalankar, D. (2018). Building resilience to climate change: Pilot evaluation of the impact of India's first heat action plan on all-cause mortality. *Journal of Environmental and Public Health, 2018*, 1–8. https://doi.org/10.1155/2018/7973519.
IITM. (2012). Climate Change Scenarios for India KeySheet 2. New Delhi, India: DEFRA-MoEF. Retrieved from India Environmental Portal.
Ji-Young, S., Lane, K., Jong-Tae, L., & Bell, M. (2016). November). Urban vegetation and heat-related mortality in Seoul, Korea. *Environmental Research, 151*, 728–733. https://doi.org/10.1016/j.envres.2016.09.001.
Lee, W., Bell, M. L., Gasparrini, A., Armstrong, B. G., Sera, F., Hwang, S., … Kim, H. (2018). Mortality burden of diurnal temperature range and its temporal changes: A multi-country study. *Environment International, 110*, 123–130. https://doi.org/10.1016/j.envint.2017.10.018.
Manoli, G., Fatichi, S., Schläpfer, M., Yu, K., Crowther, T. W., Meili, N., … Bou-Zeid, E. (2019). Magnitude of urban heat islands largely explained by climate and population. *Nature, 573*(7772), 55–60. https://doi.org/10.1038/s41586-019-1512-9.
Masoudi, M., & Tan, P. Y. (2019). Multi-year comparison of the effects of spatial pattern of urban green spaces on urban land surface temperature. *Landscape and Urban Planning, 184*, 44–58. https://doi.org/10.1016/j.landurbplan.2018.10.023.
Mavalankar, D., Shastri, P., Bandyopadhyay, T., Parmar, J., & Ramani, K. V. (2008). Increased mortality rate associated with chikungunya epidemic, Ahmedabad, India. *Emerging Infectious Diseases, 14*(3), 412–415. https://doi.org/10.3201/eid1403.070720.
Mazdiyasni, O., AghaKouchak, A., Davis, S. J., Madadgar, S., Mehran, A., Ragno, E., … Niknejad, M. (2017). Increasing probability of mortality during Indian heat waves. *Science Advances, 3*(6), e1700066. https://doi.org/10.1126/sciadv.1700066.
MoF. (2015, July 21). Re-classification/Upgradation of Cities/Towns on the basis of Cencus-2011 for the purpose of grant of House Rent Allowance to Central Government Employees. Retrieved December 10, 2018, from Department of Expenditure, Ministry of Finance, Government of India: https://doe.gov.in/sites/default/files/21-07-2015.pdf.
Mostovoy, G., King, R., Raja Reddy, K., Kakani, V. G., & Filippova, M. (2006). Statistical estimation of daily maximum and minimum air temperatures from MODIS LST data over the state of Mississippi. *GIScience & Remote Sensing, 43*(1), 78–110. https://doi.org/10.2747/1548-1603.43.1.78.
Mostovoy, G. V., King, R. L., Reddy, K. R., Kakani, V. G., & Filippova, M. G. (2006). Statistical estimation of daily maximum and minimum air temperatures from MODIS LST data over the state of Mississippi. *GIScience & Remote Sensing, 43*(1), 78–110.
Mukherjee, S., & Mishra, V. (2018). A sixfold rise in concurrent day and night-time heatwaves in India under 2 °C warming. *Scientific Reports, 8*, 16922. https://doi.org/10.1038/s41598-018-35348-w.
Neophytou, A. M., Picciotto, S., Brown, D. M., Gallagher, L. E., Checkoway, H., Eisen, E. A., & Costello, S. (2018). Exposure-lag-response in longitudinal studies: application of distributed-lag nonlinear models in an occupational cohort. *American Journal of Epidemiology, 187*(7), 1539–1548. https://doi.org/10.1093/aje/kwy019.
Oyler, J., Dobrowski, S., Holden, Z., & Running, S. (2016). Remotely sensed land skin temperature as a spatial predictor of air temperature across the conterminous United States. *Journal of Applied Meteorology and Climatology, 55*, 1441–1457. https://doi.org/10.1175/JAMC-D-15-0276.1.
Pai, D. S. (2014). Development of a new high spatial resolution (0.25° × 0.25°) long period (1901–2010) daily gridded rainfall data set over the region. *Mausam, 65*, 1–18.
Parks, R., Bennett, J., Foreman, K., Toumi, R., & Ezzati, M. (2018). National and regional seasonal dynamics of all-cause and cause-specific mortality in the USA from 1980 to 2016. *Epidemiology and Global Health*.
Revi, A., Satterthwaite, D., Aragón-Durand, F., Corfee-Morlot, J., Kiunsi, R., Pelling, M., . . . Solecki, W. (2014). Urban areas. In C. Field, V. Barros, D. Dokken, K. Mach, M. Mastrandrea, T. Bilir, . . . L. (eds.), Climate Change 2014: Impacts, Adaptation, and Vulnerability. Part A: Global and Sectoral Aspects. Contribution of Working Group II to the Fifth Assessment Report of the Intergovernmental Panel on Climate Change (pp. 535-612). Cambridge, United Kingdom and New York, NY, USA: Cambridge University Press.
Rocklöv, J., & Forsberg, B. (2008). The effect of temperature on mortality in Stockholm 1998–2003: A study of lag structures and heatwave effects. *Scandinavian Journal of Public Health, 36*(5), 516–523.
Rocklov, J., Barnett, A., & Woodward, A. (2012). On the estimation of heat-intensity and heat-duration effects in time series models of temperature-related mortality in Stockholm, Sweden. *Environmental Health, 11*, 23. https://doi.org/10.1186/1476-069X-11-23.
Rosenzweig, C., Solecki, W., Romero-Lankao, P., Mehrotra, S., Dhakal, S., Bowman, T., & Ali Ibrahim, S. (2015). ARC3.2 Summary for City Leaders. New York: Urban Climate Change Research Network, Columbia University.
Sánchez, F., Solecki, W., & Batalla, C. (2018). Climate change adaptation in Europe and the United States: A comparative approach to urban green spaces in Bilbao and New York City. *Land Use Policy, 79*, 164–173. https://doi.org/10.1016/j.landusepol.2018.08.010.
Sanderson, M., Arbuthnott, K., Kovats, S., Hajat, S., & Falloon, P. (2017). The use of climate information to estimate future mortality from high ambient temperature: A systematic literature review. *PLoS ONE, 12*(7), e0180369. https://doi.org/10.1371/journal.pone.0180369.
Steenland, K., & Armstrong, B. (2006). An overview of methods for calculating the burden of disease due to specific risk factors. *Epidemiology, 17*(5), 512–519.
Stone, B., Hess, J. J., & Frumkin, H. (2010). Urban form and extreme heat events: Are sprawling cities more vulnerable to climate change than compact cities? *Environmental Health Perspectives, 118*(10), 1425–1428.
Su, S., Zhang, Q., Pi, J., Wan, C., & Weng, M. (2016). Public health in linkage to land use: Theoretical framework, empirical evidence, and critical implications for reconnecting health promotion to land use policy. *Land Use Policy, 57*, 605–618. https://doi.org/10.1016/j.landusepol.2016.06.030.
Tobías, A., Armstrong, B., & Gasparrini, A. (2017). Investigating uncertainty in the minimum mortality temperature-methods and application to 52 Spanish Cities. *Epidemiology, 28*(1), 72–76.
Tsuboi, T. (2019). Time Zone Impact for Traffic Flow Analysis of Ahmedabad City in. Proceedings of the 5th International Conference on Vehicle Technology and Intelligent Transport Systems (VEHITS 2019) (pp. 388-395). Crete Greece: SCITEPRESS Digital Library.
Vancutsem, C., Ceccato, P., Dinku, T., & Connor, S. (2010). Evaluation of MODIS land surface temperature data to estimate air temperature in different ecosystems over Africa. *Remote Sensing of Environment, 114*(2), 449–465. https://doi.org/10.1016/j.rse.2009.10.002.
Vargo, J., Stone, B., Habeeb, D., Liu, P., & Russell, A. (2016). The social and spatial distribution of temperature-related health impacts from urban heat island reduction policies. *Environmental Science & Policy, 66*, 366–374. https://doi.org/10.1016/j.envsci.2016.08.012.
Vogel, M., Zscheischler, J., Wartenburger, R., Dee, D., & Seneviratne, S. (2019). Concurrent 2018 Hot Extremes Across Northern Hemisphere Due to Human-Induced Climate Change. *Earth's Future, 7*(7), 692–703. https://doi.org/10.1029/2019EF001189.
Wan, Z. (2014). New refinements and validation of the collection-6 MODIS land-surface temperature/emissivity product. *Remote Sensing of Environment, 140*, 36–45. https://doi.org/10.1016/j.rse.2013.08.027.
Weber, S., Sadoff, N., Zell, E., & Sherbinin, A. (2015). Policy-relevant indicators for mapping the vulnerability of urban populations to extreme heat events: A case study of Philadelphia. *Applied Geography, 63*, 231–243. https://doi.org/10.1016/j.apgeog.2015.07.006.
Wolf, T., & McGregor, G. (2013). The development of a heat wave vulnerability index for London, United Kingdom. *Weather and Climate Extremes, 1*, 59–68. https://doi.org/10.1016/j.wace.2013.07.004.
Yang, J., Hu, L., & Wang, C. (2019). Population dynamics modify urban residents' exposure to extreme temperatures across the United States. *Science Advances, 5*(12), EAAY3452. https://doi.org/10.1126/sciadv.aay3452.
Yang, J., Yin, P., Sun, J., Wang, B., Zhou, M., Li, M., … Liu, Q. (2019). Heatwave and mortality in 31 major Chinese cities: Definition, vulnerability and implications. *Science of the Total Environment, 649*, 695–702.
Yin, Q., Wang, J., Ren, Z., Li, J., & Guo, Y. (2019). Mapping the increased minimum mortality temperatures in the context of global climate change. *Nature Communications, 10*(1), 4640. https://doi.org/10.1038/s41467-019-12663-y.